JOURNAL OF MECHANICS OF CONTINUA AND MATHEMATICAL SCIENCES
www.journalimcms.org

ISSN (Online) : 2454 -7190 Vol.-15, No.-4, April (2020) pp 21-35 ISSN (Print) 0973-8975

NUMERICAL STUDY OF A THERMAL ENERGY STORAGE SYSTEM WITH DIFFERENT SHAPES INNER TUBES

Ali N. Abdul Ghafoor[1], Munther Abdullah Mussa[2]

[1,2]Department of Mechanical Engineering, College of Engineering, University of Baghdad, Iraq

[1]ali_alkassem@yahoo.com, [2]munther@coeng.uobaghdad.edu.iq

Corresponding Author: Ali N. Abdul Ghafoor

https://doi.org/10.26782/jmcms.2020.04.00003

Abstract

A numerical study to investigate the behaviour and impact of different inner tube geometric shapes on the thermal performance of the latent heat thermal energy storage (LHTES) unit have been done. Current work includes a horizontal concentric shell filling with paraffin wax as phase change material (PCM). The tested inner tube geometric shapes were circular tube, horizontal elliptical tube, and vertical elliptical tube. Finite-volume method with a single-domain enthalpy method have been used for the simulation. The results showed that the circular tube is the best due to keeping absorbing heat from PCM through HTF for a long time with 66.37% efficiency and 240.5 minutes.

Keywords: Energy storage, solidification, Shell and tube, Natural convection, PCM

I. Introduction

Energy is the key element in global development. There is a daily global demand for increasing energy. Everywhere in the world, renewable energy use is on the increases and these energy resources could be the best choice for resisting environment changes. natural sources that are responsible to generate renewable energy and these sources supply themselves and never finish. Solar, wind, and hydro-power are the most typical sources. Despite approximately getting 80 parent energy through fossil fuels, however, renewable energy which the quickest growing source of energy in the world. The urgent request for manufacturing thermal energy storage systems (TESS) came as a result to overcome problems between energy generation and energy use. Among the thermal energy storage systems are considered latent heat storage systems (LHSS) which is choosing the PCM is well suitable for these applications. A large number of studies were published dedicated to numerically and experimentally to improving and maximize the thermal performance of LHTES systems. [III], [XIII] experimentally studied the thermal behaviour of PCM in the

horizontal shell and tube. The results showed that natural convection is effective on the heat transfer for the solidification performance at the first, then after that managed by conduction. While the opposite occurs at a melting operation.[VII], [I] experimentally studied the melting/solidification of PCM in the horizontal double pipe storage unit. The results showed that natural convection controls the charging process because of buoyancy effects. While the conduction controlling the discharging process. [XI] experimentally studied LHTES unit performance of vertical shell and tube. The results showed that convection dominated in charging operations while conduction dominated in discharging operations. [XIV] experimentally studied perception the solidification behaviour in horizontal shell and tube, through changes from concentric geometry to eccentric geometries. The resultshowed that solidification time was high when using the eccentric geometries. [VI], [V] experimentally and numerically studied the comprehend convection currents that controlled from buoyancy force through the charging of the PCM in the horizontal shell and tube unit. The result showed that the melt's forehead starts the movement from a tube to the shell. Furthermore, the charging time minimized when the rising temperature for the HTF. And conduction heat transfer affects the charging while convection dominated on the discharging. [IX] numerically and experimentally studied the influence of PCM in the vertical shell and tube unit in each of the two cases, feeding HTF upper/lower in charging also repeated in discharging. The study showed the possibility of obtaining the highest efficiency in vertical units through feeding on the upper for the charging process and the opposite in discharging. [VIII] experimentally and numerically studied the influence melting/solidification of PCM in the horizontal shell and tube unit which was controlled by the thermal conduction. The results showed significant effects of HTF temperature in each charging/discharging operation of the PCM. Moreover, the radius of the tube has a high influence on the running time of the unit. [IV] Numerically studied to performance evaluation a PCM through melting inside the shell and one, two, three, and four inner tubes. The results showed the melt time of the PCM minimized with a rising quantity of tubes inside the shell. Moreover, the shell with one concentric tube required a long time for melting the PCM. [X] numerically studied using two shapes of LHTES units. The first shape as a horizontal shell and tube which PCM filling shell while, the tube using the HTF. The second shape as the opposite. The results showed that a decrease in the charging time of PCM by 50 per cent in the second shape due to the high influence of convection.

In this study, the influence of changing different inner tube geometric shapes (circular tube, horizontal elliptical tube, and vertical elliptical tube) will numerically investigate and calculate the thermal performance of the LHTES unitduring the solidification process.

II. Physical Description of Model

In the framework of this study, Fig. 1 the schematic diagram showed a concentric horizontal double pipe heat exchanger shell and tube. Which the horizontal shell of Aluminum, with outer and inner diameter 160 mm, 157 mm respectively. The thickness is 1.5 mm and 1000 mm in length. Three partitions located in the shell and

were away 200 mm, 500 mm, and 800 mm from the entrance of the shell. These partitions to study the distribution of PCM temperature, which filling the shell during the solidification process with angles 0°, 45°, and 90° respectively, along the axis. Three various geometrical shape models were used for inner concentric tubes inside the shell which the water HTF as passing through it. Model (1) is the copper circular tube with outer and inner diameter 54 mm, 51mm respectively, with 1.5 mm thickness and 1500 mm length. Model (2) is the copper horizontal elliptical tube which is the same cross-sectional area. The major diameter 60 mm and minor diameter 47.5 mm, with 1.5 mm thickness and 1500 mm length. Model (3) is the

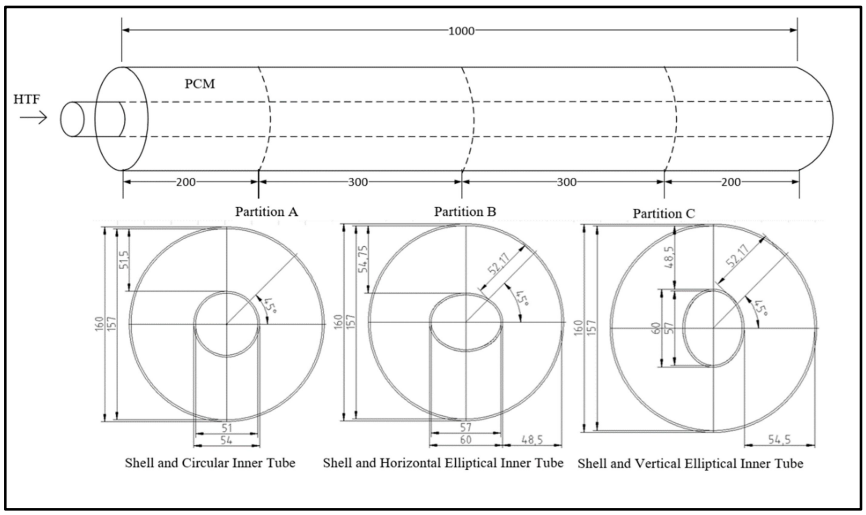

copper vertical elliptical tube which is the same dimension of a model (2). Thermo-physical properties of the PCM and other materials are recorded in table 1. Moreover, table 2 shows the number of numerical tests that chosen a constant volume flow rate at 2 L/min of HTF.

Fig. 1: Schematic Diagram of The Model.

Table 1: Thermo-Physical Properties of Used Materials.

Materials / Properties	Paraffin wax (PCM)	Water	Aluminum	Copper
Melting temperature [K]	334	-	-	-
Density in solid state [kg/m3]	894.56	-	2719	8978
Density in liquid state [kg/m3]	783.42	998.2	-	-

Specific heat in solid state [J/kg K]	1659	-	871	381
Specific heat in liquid state [J/kg K]	2460	4182	-	-
Latent heat of fusion [J / kg]	235512.5	-	-	-
Thermal conductivity in solid state [W / m K]	0.259	-	202.4	387.6
Thermal conductivity in liquid state [W / m K]	0.158	0.6	-	-
Dynamic viscosity [kg/m s]	0.01405	0.001003	-	-
Solidus temperature [K]	318.5	-	-	-
Liquidus temperature [K]	339	-	-	-
Thermal expansion coefficient [1/K]	0.000307	-	-	-

Table 2:Number of Tests

Geometrical Shapes Models	Volume Flow Rate of Water L / min	Velocity m / sec	Reynolds Number
Circular Tube	**2**	**0.01631**	**952.363**
Horizontal Elliptical Tube	**2**	**0.0172**	**978.024**
Vertical Elliptical Tube	**2**	**0.0172**	**978.024**
Total Number of Tests	**3**		

III. Summarization of Calculations

The instantaneous energy q_{ch}&q_{dis} and the energy of accumulative $Q_{ch\,\&\,dis}$depends on the inlet and outlet temperatures of water as the heat transfer fluid from the thermal energy storage system through charging or discharging. The equations can be articulated using which was described by [V] as below:

$$q_{ch} = \dot{m}\, C_p(T_{in} - T_{out}) \quad (1)$$

$$q_{dis} = \dot{m}\, C_p(T_{out} - T_{in}) \quad (2)$$

$$Q_{ch\,\&\,dis} = \sum q_{ch\,\&\,dis}\, \Delta t \quad (3)$$

Where ($\dot{m}$) represented the mass flow rate of HTF, (c_p) is the specific heat capacity of HTF, (T_{in}&T_{out}) are inlet/outlet of the HTF temperatures respectively, and Δt is the time. In converse to steady-state operations where we observe in the transient

state operations, the energy accumulative charge/discharge ($Q_{ch\ \&\ dis}$) by HTF with ($Q_{PCM,ch\ \&\ dis}$) of phase change material are not equal; which are components of the heat that are interchanged through the parts of a heat exchanger system. These equations can be written as below:

$$Q_{H.E,ch} = M_{H.E}C_{p,H.E}(T_{en} - T_{ini}) \quad (4)$$

$$Q_{H.E,dis} = M_{H.E}C_{p,H.E}(T_{ini} - T_{end}) \quad (5)$$

Where ($M_{H.E}$) represented the mass of the heat exchanger, ($C_{p,H.E}$) is the specific heat capacity of the heat exchanger, and (T_{ini}&T_{end}) are start/end of the phase change materialtemperatures of processing respectively. And the accumulative energy exchangeable with the phase change material ($Q_{PCM,ch\ \&\ dis}$) can be written as below:

$$Q_{PCM,ch\ \&\ dis} = Q_{ch\ \&\ dis} - Q_{H.E,ch\ \&\ dis} \quad (6)$$

And to estimate the consequence theoretical efficiency of the LHTES system which can be written as below:

$$\eta_{\text{theory}} = \frac{Q_{PCM,ch\ \&\ dis}}{Q_{max,ch\ \&\ dis}} \quad (7)$$

The maximum quantity of the theoretical energy ($Q_{max,ch\ \&\ dis}$) through charging/discharging operation as an equivalent of the total energy received or given from the phase change material which can be written as below:

$$Q_{max,ch} = M_{PCM[C_{P,PCM}(T_{ini} - T_{solidus}) + (L*f) + C_{P,PCM}(T_{end} - T_{liquidus})]} \quad (8)$$

$$Q_{max,dis} = M_{PCM[C_{P,PCM}(T_{ini} - T_{liquidus}) + (L*f) + C_{P,PCM}(T_{liquidus} - T_{solidus})]} \quad (9)$$

Where the (M_{PCM}) is the mass of phase change material, ($C_{P,PCM}$) is the specific heat capacity of phase change material, ($T_{liquidus}, T_{solidus}$) are the liquidus and solidus temperature of phase change material, (L) is the latent heat of fusion, and (f) is the liquid fraction.

IV. Mathematical Model and Numerical Simulation

A mathematical model and numerical simulation of the present study, which is the influence of the changing inner geometric shapes on the heat transfer mechanism from PCM to HTF during solidification operations. The numerical simulation was done by the help of a computational fluid dynamic program tool which is the commercial package of ANSYS-Fluent 19.2. The simulation for the solidification operation of a PCM is modeled with an enthalpy-method which described by [II], [XII]. This method technique avoids discontinuity and the balance of energy at the solid/liquid interface. Also, there is no explicitly tracking for the interface of solid-liquid, but it depends on the liquid fraction (f). The assumptions which have been considered in the analysis are:

1. Unsteady state condition.
2. Laminar flow for HTF.

3. Incompressible flow for HTF (ρ=Constant) and Newtonian fluid.
4. Three-dimensional flow.
5. The PCM is homogeneous and isotropic.
6. The term of viscous dissipation is considered negligible.
7. The entering temperature of HTF constant at 299 K.
8. The outer surface of the shell is perfectly insulated, so there is no loss in heat transfer to the surrounding, and heat transfer occurs between the PCM and HTF only.

The energy equation is shown the expression of the temperature and total volumetric enthalpy:

$$\frac{\partial \rho H}{\partial t} + \nabla . (\rho v H) = \nabla . (k \nabla T) + S \tag{10}$$

Where (ρ) is the density of the PCM, (ν) the velocity, (H) total volumetric enthalpy which represents the combined both sensible and latent heats, k as a thermal conductivity, and S which is the source term.

$$H = h + f_L \tag{11}$$

$$h = h_{ref} + \int_{T_{ref}}^{T} C_p dT \tag{12}$$

where the (C_p) and (f) represents the specific heat capacity and liquid fraction respectively. And (T_{ref})represent the reference temperature ($299K$).

The region of a mushy zone as represented as below:

$$f = \begin{cases} 0 & \text{when} \quad T < T_{solidus} \\ \dfrac{T - T_{solidus}}{T_{liquidus} - T_{solidus}} & \text{when} \quad T_{solidus} \le T \le T_{liquidus} \\ 1 & \text{when} \quad T > T_{liquidus} \end{cases} \tag{13}$$

After compensation (11) - (13) into the equation (10) the energy equation written as:

$$\frac{\partial \rho h}{\partial t} + \nabla . (\rho v h) = \nabla . (k \nabla T) - \frac{\partial \rho f_L}{\partial t} - \nabla . (\rho v f_L) + S \tag{14}$$

Where L as the heat fusion of latent, and the momentum equation will be written as:

$$\frac{\partial \rho v}{\partial t} + \nabla . (\rho v v) = - \nabla P + \nabla . (\mu \nabla v) + \rho g + \frac{(1-f)^2}{f^3 + \varepsilon} v A_{mush} \tag{15}$$

Where A_{mush} (10^5) is the mushy zone constant which acts as a damping factor of the velocity during the solidification of the PCM, and ε equal (0.001) is a tiny number to forbid division by zero.

The Boussinesq approximation is used because of the difference of tiny density. Assumed that the fluid density is constant along with terms of the momentum equation not including a term of body force, and it is modeled established as reference density (ρ_0), temperature (T_0), thermal expansion coefficient (β).

Then the momentum equation will be written as:

$$\frac{\partial \rho_0 \nu}{\partial t} + \nabla.(\rho_0 \nu\nu) = -\nabla P + \nabla.(\mu \nabla \nu) + (\rho - \rho_0)g + \frac{(1-f)^2}{f^3+\varepsilon} \nu A_{mush} \quad (16)$$

$$(\rho - \rho_0)g = -\rho_0 \beta (T - T_0) \quad (17)$$

And the continuity equation will be written as:

$$\frac{\partial \rho}{\partial t} + \nabla.(\rho v) = 0 \quad (18)$$

Numerical Setup

A quarter of the shell and tube will be analyzed and this will reduce computational domain and analysis time by 75%. To improve the results of numerical simulation and reduce the error rate. The mesh independent test was done by selecting five different numbers of model mesh elements with the mass fraction to choose the appropriate one that not leads to divergence calculations. Fig. 2,3 shows the mesh independent test result and mesh grid for geometric shapes respectively. According to the results, the mesh element size of a quarter shapes included shell and circular tube, shell and horizontal elliptical tube, and shell and vertical elliptical tube were 183800, 178050, and 180250 respectively. PCM initialization temperature has been set at 345 K. Different time step sizes were tested in which the best result was obtained with a 0.05 sec time step size. The set value for the maximum iteration per time step was 10 to ensure solution convergence for each step and the number of time steps was 4,000,000. The SIMPLE algorithm had been selected for pressure-velocity coupling. While a second-order upwind discretization of momentum and energy equations were used, and second-order for pressure energy equation. Also, first-order implicit for the transient formulation. The under-relaxation factors for pressure, density, body forces, momentum, liquid fraction update, and energy are considered to be 0.3, 1, 1, 0.7, 0.9 and 1 respectively.

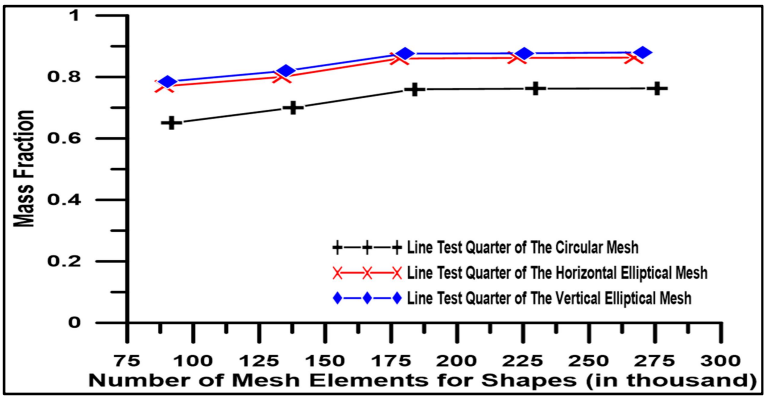

Fig. 3: Mesh Independent Test Result.

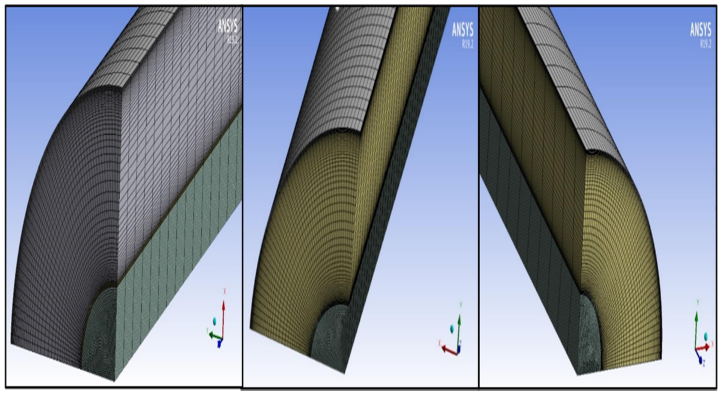

shell and circular tube shell and horizontal elliptical tube shell and vertical elliptical tube

Fig. 3: Mesh Grid For Geometric Shapes.

V. Results and Discussion

After setting the PCM melting initialization temperature has been set at 345 K, the discharging process starts through passing the cold water at a constant temperature at 299 K. This procedure is repeated when replacing the inner geometric shapes (Circular tube, Horizontal elliptical tube, and Vertical elliptical tube) for each simulation test. The results showed acceptable values for each case in the numerical solution. The CPM average mass fraction (AMF) contours with values 1, 0.75, 0.5, and 0.25 in Fig. 4 for all the geometric shapes during a discharging process. The figures indicate that the heat transfer between HTF and the liquid of PCM was governed by natural convection which was very fast in the beginning. The speed of heat exchange lead to the solidification PCM layer near the HTF tube that moving away from the HTF tube to the shell. The speed and priority of solidification start from the horizontal axis with an angle at 0°, the inclined axis with an angle at 45°, then the vertical axis with an angle at 90°. Due to the lower thermal conductivity and growing the solidification layer thickness of the PCM near the HTF wall lead to increased solidification time. The heat transfer through natural convection happened due to the buoyancy force, but after that, the heat transfer was controlled by the conduction and that lead to the result of extending the solidification time period.

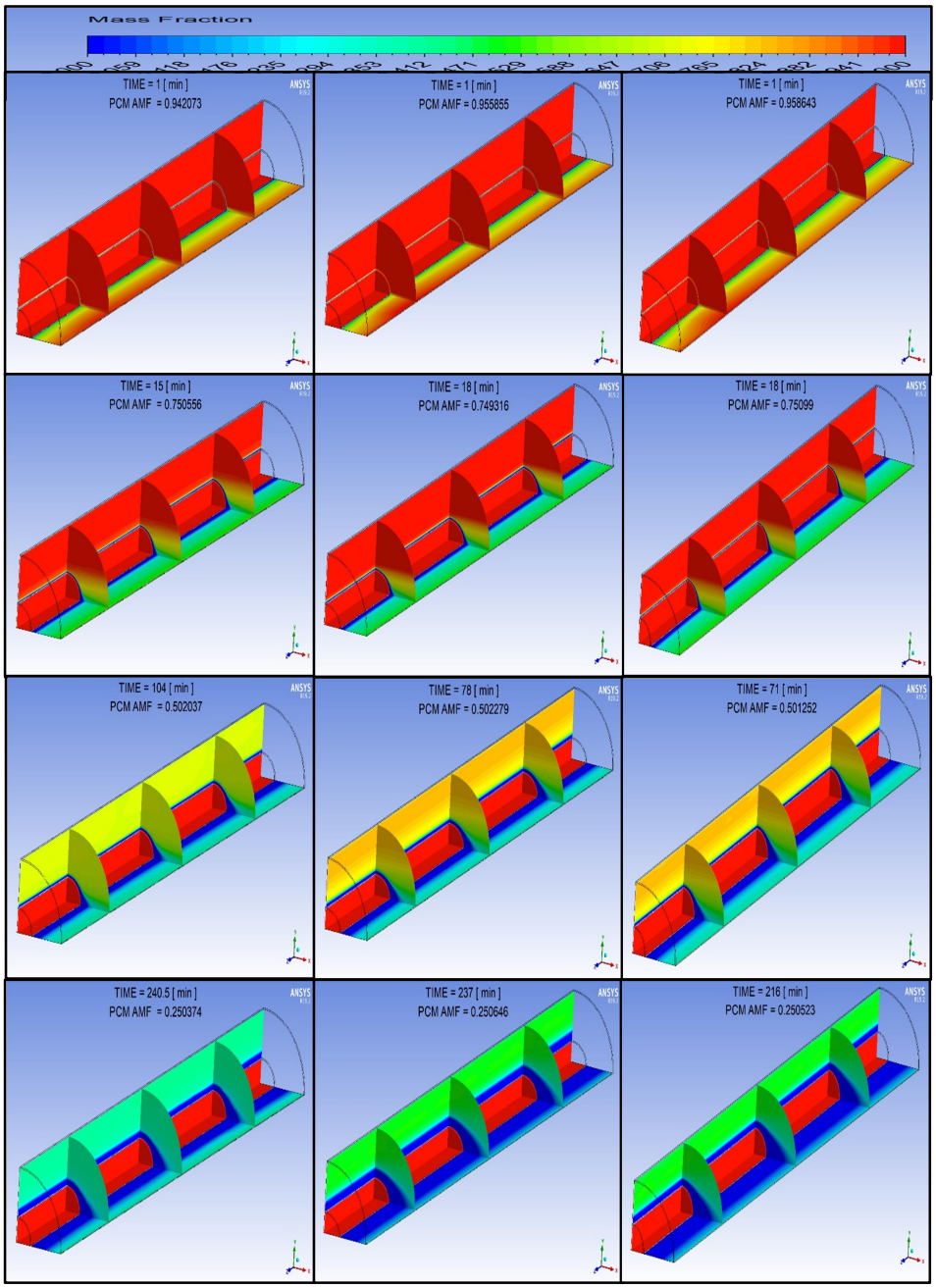

Shell and Circular Tube Shell and Horizontal Elliptical Tube Shell and Vertical Elliptical Tube

Fig. 4: Mass Fraction for Three Geometric

Shapes at 2 L/min of HTF During Discharging Process.

The Distribution of PCM Temperature along the Axes

Fig. 5 shows the numerical and experimental temperature distribution for shell and (Circular tube, Horizontal elliptical tube, and Vertical elliptical tube) along the axis. Shell and Circular tube at the beginning of solidification when the liquid fraction was 0.942, the temperatures drop at the vertical and inclined axes at the same values while these values drop fast at the horizontal axis. Moreover, the temperatures drop at partition A more than partition B and partition C due to the large heat transfer between PCM and HTF in the first part of the shell and circular tube. Increase temperature drop of the PCM with time in all partitions until the liquid fraction reached 0.25 where it appears clearly that the solidification is on the horizontal axis first then inclined axis and vertical axis. The same thing saw and repeated and with the other two models but, the PCM solidification with time was faster in the shell and vertical elliptical tube followed by the shell and horizontal elliptical tube then after that the shell and circular tube.

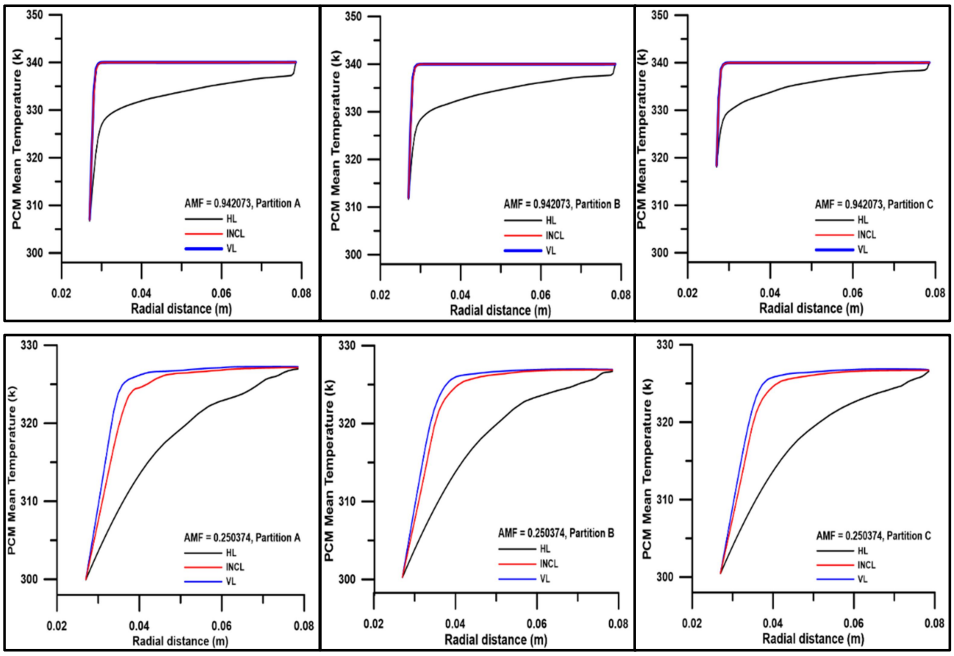

Shell and Circular Tube.

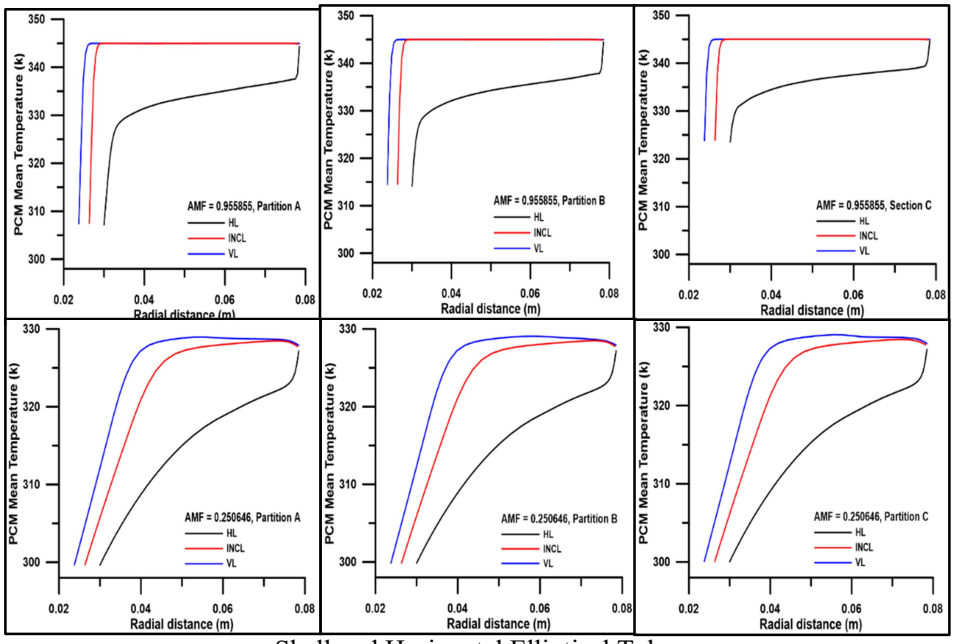

Shell and Horizontal Elliptical Tube.

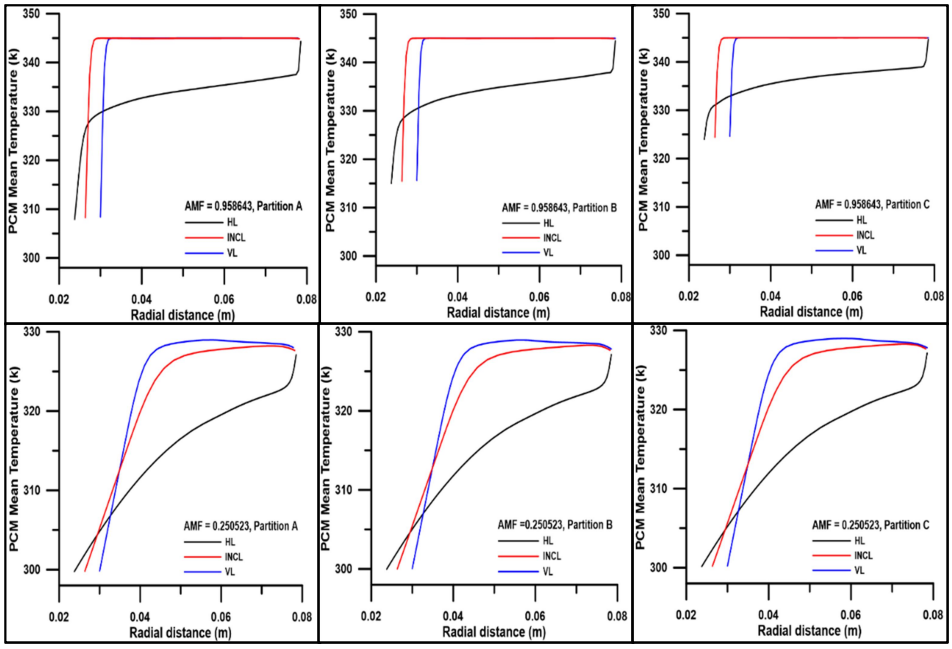

Shell and Vertical Elliptical Tube.

Fig. 5: Numerical and Experimental Temperature Distribution for Three Geometric Shapes During Discharging Process.

Heat Transfer Rate Gained

Fig. 6 shows the heat transfer gained from the HTF through PCM solidification. which referred that the maximum heat transfer gained with shell and circular tube at 0.25 of liquid fraction was 1123.379 kj at 240.5 minutes. With the same liquid fraction, 836.874 kj at 237 minutes was the heat transfer gained from the PCM to the HTF in the shell and horizontal elliptical tube. The last geometrical shape of the shell and vertical elliptical tube was 749.762 kj at 216 minutes of the heat transfer gained from the PCM to the HTF.

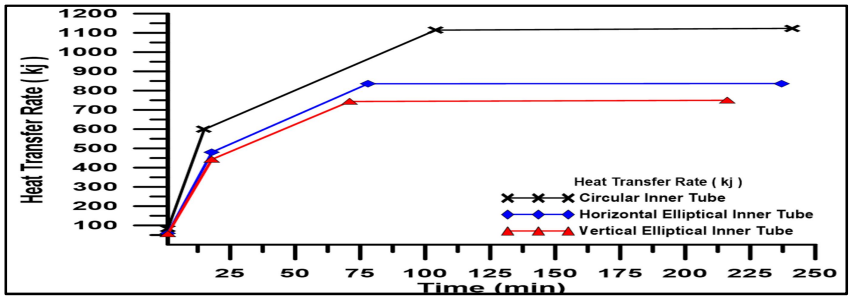

Fig. 6: heat transfer gained from the HTF During Discharging Process.

Cumulative Energy Exchanged with PCM

Fig. 7 shows the cumulative energy exchanged with PCM in the solidification process for the shell and three different shape geometry. The curves showed that the largest cumulative energy in the shell and the circular tube with 0.25 liquid fraction was 1049.546 kj at 240.5 minutes. With the same liquid fraction, 762.322 kj at 237 minutes was the cumulative energy in the shell and horizontal elliptical tube. While the last geometrical shape of the shell and vertical elliptical tube was 675.383 kj at 216 minutes was the cumulative energy.

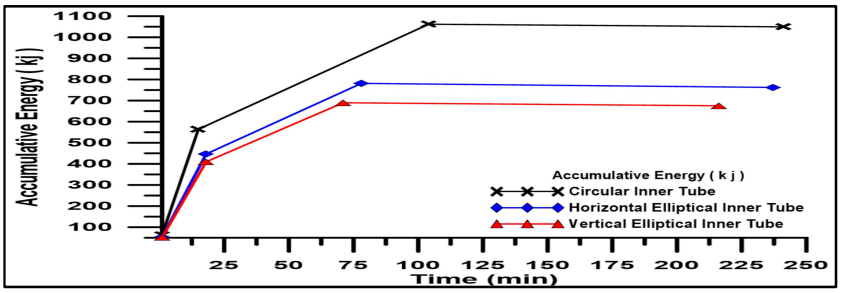

Fig. 7: Cumulative Energy Exchanged with PCM During Discharging Process.

Thermal Performance

Fig. 8 shows the combination of theoretical thermal efficiency for the shell and three different shapes geometry during solidification with time. The curves

showed that the largest thermal efficiency was in the shell and the circular tube with 66.37% at 240.5 minutes. Followed by 48.21% at 237 minutes of thermal efficiency for the shell and horizontal elliptical tube.While 42.72% at 216 minutes of thermal efficiency for the shell and vertical elliptical tube.

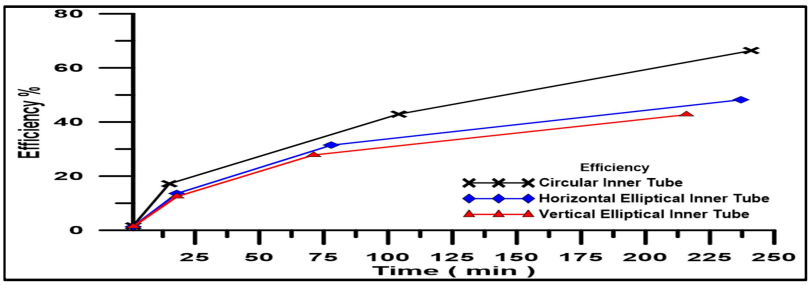

Fig. 8: Theoretical and Experimental Thermal Efficiency During Discharging Process.

VI. Conclusions

Depending on the achieved numerical simulation on the influence of changing the inner tube geometric shapes (circular tube, horizontal elliptical tube, and vertical elliptical tube) on the thermal performance of the LHTES unit during the solidification process. Several conclusions have been extracted:

Through the solidification process of the PCM, a recognized the common relationship between two important methods of heat transfer which are natural convection and conduction heat transfer in the shell and all different inner tube geometric shapes. The fast convection currents which govern the PCM solidification process a result of the influence of buoyancy force in the first, then controlled by conduction heat transfer, which that needs more time to finish the solidification process.

Both the heat transfer gained and cumulative energy exchanged were higher for the shell and the circular tube and an efficiency record of 66.37 % at 0.25 liquid fraction during 240.5 minutes. The horizontal elliptical tube and the vertical elliptical tube came behind the previous shape. The geometrical shape nature explained the slow response in the time required for the solidification process as a result of the far distance between the center of the tube and the circular wall compared to other shapes.

VII. Acknowledgment

We gratefully acknowledge the Ministry of Higher Education and Scientific Research/University of Baghdad for its support.

References

I. Agarwal, Ashish, and R. M. Sarviya. 2016. "An Experimental Investigation of Shell and Tube Latent Heat Storage for Solar Dryer Using Paraffin Wax as Heat Storage Material." *Engineering Science and Technology, an International Journal* 19 (1): 619–31. https://doi.org/10.1016/j.jestch.2015.09.014.

II. Al-Abidi, Abduljalil A., Sohif Bin Mat, K. Sopian, M. Y. Sulaiman, and Abdulrahman Th Mohammed. 2013. "CFD Applications for Latent Heat Thermal Energy Storage: A Review." *Renewable and Sustainable Energy Reviews* 20: 353–63. https://doi.org/10.1016/j.rser.2012.11.079.

III. Avci, Mete, and M. Yusuf Yazici. 2013. "Experimental Study of Thermal Energy Storage Characteristics of a Paraffin in a Horizontal Tube-in-Shell Storage Unit." *Energy Conversion and Management* 73: 271–77. https://doi.org/10.1016/j.enconman.2013.04.030.

IV. Esapour, M., M. J. Hosseini, A. A. Ranjbar, Y. Pahamli, and R. Bahrampoury. 2016. "Phase Change in Multi-Tube Heat Exchangers." *Renewable Energy* 85: 1017–25. https://doi.org/10.1016/j.renene.2015.07.063.

V. Hosseini, M. J., M. Rahimi, and R. Bahrampoury. 2014. "Experimental and Computational Evolution of a Shell and Tube Heat Exchanger as a PCM Thermal Storage System." *International Communications in Heat and Mass Transfer* 50: 128–36. https://doi.org/10.1016/j.icheatmasstransfer.2013.11.008.

VI. Hosseini, M. J., A. A. Ranjbar, K. Sedighi, and M. Rahimi. 2012. "A Combined Experimental and Computational Study on the Melting Behavior of a Medium Temperature Phase Change Storage Material inside Shell and Tube Heat Exchanger." *International Communications in Heat and Mass Transfer* 39 (9): 1416–24. https://doi.org/10.1016/j.icheatmasstransfer.2012.07.028.

VII. Jesumathy, S. P., M. Udayakumar, S. Suresh, and S. Jegadheeswaran. 2014. "An Experimental Study on Heat Transfer Characteristics of Paraffin Wax in Horizontal Double Pipe Heat Latent Heat Storage Unit." *Journal of the Taiwan Institute of Chemical Engineers* 45 (4): 1298–1306. https://doi.org/10.1016/j.jtice.2014.03.007.

VIII. Kibria, M. A., M. R. Anisur, M. H. Mahfuz, R. Saidur, and I. H.S.C. Metselaar. 2014. "Numerical and Experimental Investigation of Heat Transfer in a Shell and Tube Thermal Energy Storage System." *International Communications in Heat and Mass Transfer* 53: 71–78. https://doi.org/10.1016/j.icheatmasstransfer.2014.02.023.

IX. Longeon, Martin, Adèle Soupart, Jean François Fourmigué, Arnaud Bruch, and Philippe Marty. 2013. "Experimental and Numerical Study of Annular PCM Storage in the Presence of Natural Convection." *Applied Energy* 112: 175–84. https://doi.org/10.1016/j.apenergy.2013.06.007.

X. Mahdi, Mustafa S., Hameed B. Mahood, Ahmed F. Hasan, Anees A. Khadom, and Alasdair N. Campbell. 2019. "Numerical Study on the Effect of the Location of the Phase Change Material in a Concentric Double Pipe Latent Heat Thermal Energy Storage Unit." *Thermal Science and Engineering Progress* 11: 40–49. https://doi.org/10.1016/j.tsep.2019.03.007.

XI. Rathod, M. K., and J. Banerjee. 2014. "Experimental Investigations on Latent Heat Storage Unit Using Paraffin Wax as Phase Change Material." *Experimental Heat Transfer* 27 (1): 40–55. https://doi.org/10.1080/08916152.2012.719065.

XII. Seddegh, Saeid, Xiaolin Wang, and Alan D. Henderson. 2016. "A Comparative Study of Thermal Behaviour of a Horizontal and Vertical Shell-and-Tube Energy Storage Using Phase Change Materials." *Applied Thermal Engineering* 93: 348–58. https://doi.org/10.1016/j.applthermaleng.2015.09.107.

XIII. Senthil, Ramalingam, and Marimuthu Cheralathan. 2016. "Melting and Solidification of Paraffin Wax in a Concentric Tube PCM Storage for Solar Thermal Collector." *International Journal of Chemical* 14 (4): 2634–40. http://www.tsijournals.com/abstract/melting-and-solidification-of-paraffin-wax-in-a-concentric-tube-pcm-storage-for-solar-thermal-collector-12762.html.

XIV. Yazici, Mustafa Yusuf, Mete Avci, Orhan Aydin, and Mithat Akgun. 2014. "On the Effect of Eccentricity of a Horizontal Tube-in-Shell Storage Unit on Solidification of a PCM." *Applied Thermal Engineering* 64 (1–2): 1–9. https://doi.org/10.1016/j.applthermaleng.2013.12.005.